

Simplified VH equations for foundation punch-through sand into clay

J.-C. Ballard, P. Delvosal & P.H. Yonatan
Fugro Engineers S.A. / N.V., Brussels, Belgium

A. Holeyman
Université Catholique de Louvain, Belgium

S. Kay
Fugro Engineers B.V., Leidschendam, The Netherlands

ABSTRACT: This paper gives simplified VH equations for surface strip foundation punch-through sand into uniform clay derived from 2D plane strain numerical simulations using Limitstate:GEO. The equations have been calibrated in the engineering ranges normally encountered in geotechnical engineering practice and have been inserted into proprietary computer program ISOBARE for everyday use.

1 INTRODUCTION

The assessment of bearing capacity of surface foundations on layered soils and subjected to combined VH loading is a common problem in the industry. For pure V loading, reliable analytical solutions are available. Of these, the “load spread” method (Young and Focht, 1981) is popular, in spite of the difficulty in selecting an appropriate “load spread factor”. For combined VH loading, reliable analytical solutions are scarce, especially for the most common offshore punch-through problem, sand over clay. Depending on the assumption made regarding horizontal load transfer, optimistic or pessimistic VH yield surfaces can result.

2 ANALYTICAL SOLUTIONS

2.1 Pure vertical loading

Several analytical approaches are available to estimate the bearing capacity of sand overlying clay. Of these, the “load spread” method is frequently used.

In this approach, it is assumed that the sand acts to spread the load and that the bearing capacity failure occurs within the clay. The load spread mechanism within the sand layer is modeled relatively simply by assuming that the vertical stresses associated with the footing load are confined to a zone defined by lines at angle β to the vertical, as shown on Figure 1.

Load from the footing is assumed to be distributed uniformly over a width B' at the base of the sand layer, where $B' = B + 2D \tan \beta$. For uniform clay, the bearing capacity V (or bearing pressure v) of the footing may be estimated using the following expression:

$$V = Bv = B'(s_u N_c + q) - W \quad (1)$$

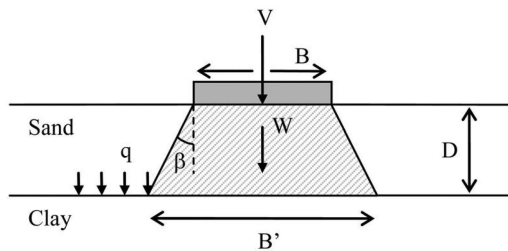


Figure 1. Load spread mechanism.

where s_u = clay undrained shear strength; N_c = standard bearing capacity factor for undrained loading; q = sand surcharge ($= \gamma D$); and W = weight of sand confined in the load spread zone. It should be noted that the β angle implicitly accounts for any shear forces acting on the sides of the load spreading body.

The problem with this method is that the chosen value of β can have an important influence on the calculated bearing capacity. A value of β between $\tan^{-1}(1/3)$ and $\tan^{-1}(1/5)$ is often adopted in practice (Kellezi, 2009) although it is generally accepted that the value of this parameter is influenced by the strength of the sand, the strength of the clay and the geometry of the problem. The use of these standard values may lead to results on the unsafe side in certain situations.

2.2 Combined VH loading and yield surface

For combined VH loading, analytical solutions are scarce for the sand over clay case, which is commonly encountered offshore. Two extreme assumptions can be made. The first assumes that the bearing capacity of the clay layer is not influenced by the horizontal load, namely, the horizontal load is fully taken by the sand

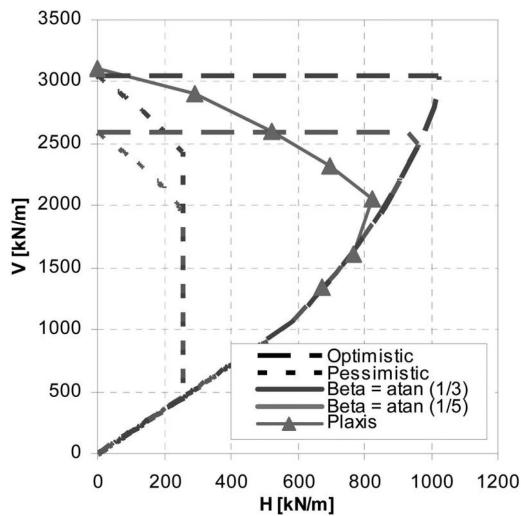


Figure 2. Comparison between simplified assessments and finite element modeling for strip footing on sand over clay.

layer. The opposite one is to assume that the horizontal load is fully transferred to the clay layer, namely the sand layer does not take any horizontal load. Depending on the assumptions made, optimistic or pessimistic VH yield surfaces can result, as illustrated in the example presented in the next Section.

2.3 Reference problem

The engineering example that initiated this research is presented. The offshore spudcan foundation was circular with a 14 m diameter. Soil conditions consisted of a 8.5 m thick loose sand layer ($\gamma' = 9.5 \text{ kN/m}^3$, $\phi' = 29^\circ$) overlying soft clay ($s_u [\text{kPa}] = 18 + 1.6z$ [m], where z is the depth from top of clay layer).

As a first approach, the foundation was treated as an infinite strip so that the analytical approaches discussed above could be directly compared with a 2D plane strain finite element simulation using Plaxis 2D v9 (Plaxis, 2002) and fully associated flow.

The results of the comparison are shown on Figure 2. In this particular situation, a load spread angle β of $\tan^{-1}(1/3)$ is appropriate for pure vertical bearing capacity, which would be underestimated with $\beta = \tan^{-1}(1/5)$. With regard to the VH yield surface, it is either optimistic or extremely cautious depending on the assumption made with regard to horizontal load transfer (see Section 2.2). The conventional sand equations (Brinch-Hansen, 1970) are seen to be reasonable in the lower part of the VH yield surface (i.e. region where $V < 200 \text{ kN/m}$), where sliding and general shear failure in sand dominate.

3 NUMERICAL MODELING

3.1 Introduction

Numerical simulations were performed to determine the bearing capacity of strip footings on sand over

uniform clay under pure V load and combined VH loading for a series of cases that cover the engineering ranges normally encountered in offshore geotechnical practice.

Dimensionless groups were used to limit the number of analyses. The bearing pressure v may be shown to be given by the functional form (Michalowski et al, 1995):

$$\frac{v}{\gamma B} = f\left(\frac{D}{B}, \frac{s_u}{\gamma D}, \phi'\right) \quad (2)$$

where γ = sand unit weight; and ϕ' = sand friction angle.

The VH curves were numerically derived for the following cases:

- $D/B = 0.25, 0.5, 0.75$ and 1
- $s_u/\gamma D = 0.25, 0.5, 1, 2$ and 4
- $\phi' = 25, 30, 35$ and 40°

3.2 Software

Commercial programs Plaxis 2D v9 and Limitstate:GEO v2 (Limitstate, 2009) were used for these simulations.

Limitstate:GEO (LSG) is very recent. It is designed to rapidly analyze the ultimate limit (or "collapse") state for a wide variety of geotechnical problems. The soil failure model is rigid perfectly plastic (Tresca/Mohr-Colomb) with fully associated flow rule. The current version is limited to 2D plane strain analyses; extension to axisymmetry is under development and planned to be released shortly. LSG directly determines the ultimate limit state using the Discontinuity Layout Optimization (DLO) algorithm (Smith & Gilbert, 2007). DLO involves the use of rigorous mathematical optimization techniques to identify a critical layout of lines of discontinuity which form at failure. These lines of discontinuity are typically 'slip-lines' in planar geotechnical stability problems and define the boundaries between the moving rigid blocks of material that makeup the collapse mechanism. Associated with this mechanism is a collapse load factor, which will be an upper bound relative to the 'exact' load factor according to formal plasticity theory. Thus in essence the procedure replicates and automates traditional upper bound manual limit analysis. Solution accuracy can be improved by increasing the density of nodes covering the body under consideration, which in turn increases the number of discontinuities available for possible inclusion in the critical mechanism.

3.3 Comparison of results

The two programs were first evaluated by performing simulations in homogeneous isotropic soil conditions and comparing the results for vertical bearing capacity with classical analytical solutions.

Highly accurate solutions have been obtained with both programs for bearing capacity in purely cohesive

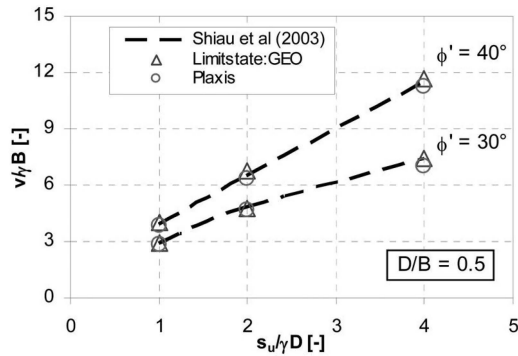


Figure 3. Bearing capacity of strip footing on sand over clay, comparison of results. Note that x-axis is $s_u/\gamma D$, not $s_u/\gamma B$.

(Tresca) material. Bearing capacity in frictional media (with Mohr-Coulomb failure criteria) were found to be more challenging for both programs, although results within about 10%, compared to Martin's exact solution (Martin, 2005), could be found, which is acceptable for this latter type of problem.

Some of the cases published by Shiau et al (2003) were verified for the sand over clay problem. Shiau used finite element formulations of the limit analysis theorems to obtain rigorous plasticity solutions for the bearing capacity of a layer of sand on clay. As shown on Figure 3, both programs were able to reproduce reasonably well Shiau et al's results.

3.4 Plaxis Vs. Limitstate:GEO

As expected for surface foundations on sand, numerical problems were encountered with Plaxis. A phenomenon called "apparent strain softening" develops just next to the footing. As any softening phenomenon, the solution becomes very sensitive to mesh. Convergence was slow and "load-settlement" curves were irregular, the roughness increasing with increasing ϕ' . Our experience is that the problem is aggravated by mesh refinement while unrealistic failure modes emerge next to the footing.

LSG was more robust and reliable. Results converged steadily towards analytical solutions by increasing the density of nodes. Solutions within 10% tolerance could generally be obtained within a few minutes compared to several hours with Plaxis. Therefore, LSG was found to be the most appropriate tool for our ultimate load problem.

3.5 Influence of non-associativity

An advantage of the finite element method is that the influence of non-associativity in sand may be investigated while fully associated flow is assumed in LSG.

It is generally believed that the assumption of fully associated flow rule in sand is reasonable for unconfined problems such as the bearing capacity of shallow foundations. Zienkiewicz et al (1975) published numerical simulations, assuming fully associated and

non-associated flow rules, showing almost no difference in the results. However, these simulations were performed for small friction angles ($\phi' < 30^\circ$). Loukidis et al (2009) recently published finite element simulations showing that the difference becomes more significant for higher friction angles ($\phi' > 30^\circ$). They observed that the bearing capacity is 10–30% smaller (than when $\psi = \phi'$) when realistic pairs of ϕ' - ψ values are assumed. The higher ϕ' , the higher the difference.

The difference was found by the Authors of this paper to be less significant (5–15%) for the sand over clay case. This was expected as the failure mechanism in that case is only partly located in the sand layer.

Errors of 5–15% tend to be masked by the fact that the bearing capacity factor N_γ in sand is highly sensitive to ϕ' value. Indeed, an error of 5–15% corresponds to assuming an angle of friction less than 1° smaller in an associated flow model. Therefore, the analyses were performed assuming associated flow.

4 RESULTS AND DISCUSSION

4.1 Vertical bearing capacity

LSG results for the vertical bearing capacity are given in Figure 4. In this paper, typical results for the D/B ratios of 0.5 and 1 are shown. Although no exact solutions are available, it is our opinion that, based on work of others and LSG cases where model geometry and nodal refinement were optimized, these results may in certain cases slightly overestimate the exact solution (up to about 10%).

As expected, the normalized vertical bearing capacity increases with increasing $s_u/\gamma D$, ϕ' and D/B. As the undrained shear strength of the clay increases, the curves flatten out for small friction angles and the failure mechanism becomes concentrated in the sand layer.

Typical failure mechanisms observed are illustrated on Figure 5 for two specific cases. The first case is a dense sand layer overlying soft clay. The assumption of the load spread mechanism seems appropriate in this case. On the other hand, for the case of loose sand on stiffer clay, the assumption of a load spread mechanism with traditionally used load spread angles would lead to a severe overestimation of bearing capacity.

The results from the parametric study are plotted in an alternative way in Figure 6 in order to illustrate the load spread mechanisms within the sand layer. In this plot, the parameter β is back-calculated using the standard expressions presented in Section 2. This load spread model is based on a highly simplified view of the mechanics of the system, hence particular β values do not have a precise physical interpretation. The load spread model becomes inappropriate when failure is confined to the sand layer, and so Figure 6 presents only results where failure occurred in sand and clay. Figure 6 also includes results for D/B ratios of 0.25 and 0.75.

The results show that β is (1) remarkably insensitive to the value of D/B, (2) even more remarkably

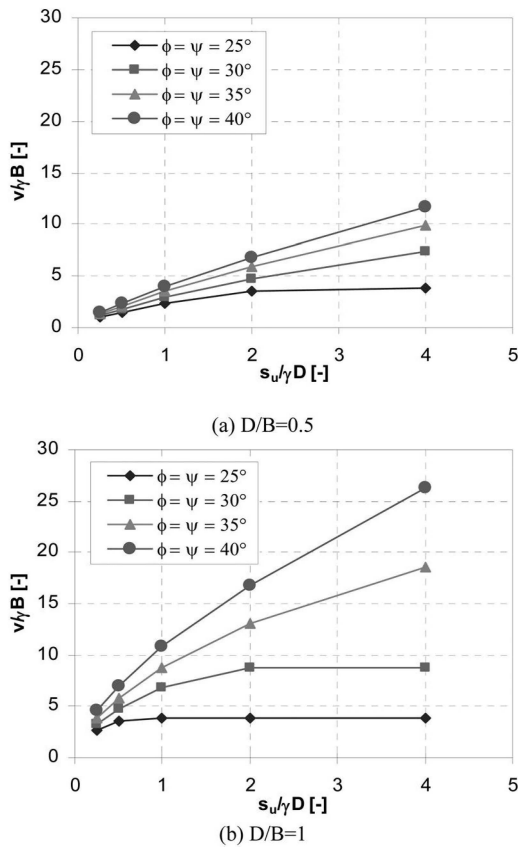


Figure 4. Limitstate:GEO results, variation of $v/\gamma B$ with $s_u/\gamma D$ for (a) $D/B = 0.5$ and (b) $D/B = 1$.

varying linearly with the logarithm of $s_u/\gamma D$ and (3) varying approximately linearly with friction angle ϕ' for a given $s_u/\gamma D$. The equivalent load spread angle β decreases with decreasing sand friction angle and increasing undrained shear strength ratio $s_u/\gamma D$.

For sand over normally consolidated clay ($s_u/\gamma D \sim 0.25$), the values traditionally used for β (i.e. 11 and 18°) are cautious. However, they may become unsafe when the clay undrained shear strength increases: equivalent β values can even become negative.

4.2 VH yield surfaces

The computed VH yield surfaces are presented on Figure 7 for one D/B ratio (0.5) and one sand friction angle (35°). The upper part of the yield surfaces are clearly curved so that the assumption of a flat top part (see Figure 2) is unconservative. A typical failure mechanism for inclined loading is shown on Figure 8.

5 SIMPLIFIED EQUATIONS

5.1 Introduction

Simplified equations derived from the 2D plane strain numerical results presented above are proposed. These

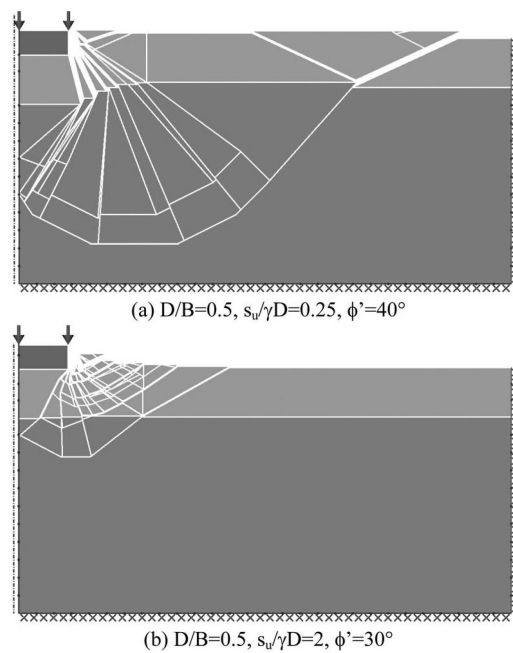


Figure 5. Limitstate:GEO failure mechanisms for $D/B = 0.5$ (a) dense sand over soft clay: $s_u/\gamma D = 0.25$, $\phi' = 40^\circ$ and (b) loose sand over stiff clay: $s_u/\gamma D = 2$, $\phi' = 30^\circ$.

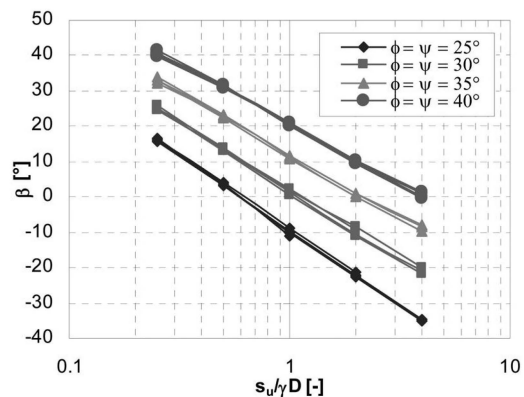


Figure 6. Variation of equivalent β with $s_u/\gamma D$ for $D/B = 0.25, 0.5, 0.75$ and 1.

equations can be used to compute VH yield surfaces of surface strip foundations on sand over uniform clay.

5.2 Pure vertical loading

When assessing the bearing capacity of shallow foundations on sand over clay, the results presented in section 4 showed that the load spread angle need not be an input variable. A relationship that computes automatically the appropriate load spread angle can easily be found: β is essentially independent of D/B and linearly varying with the logarithm of $s_u/\gamma D$, and

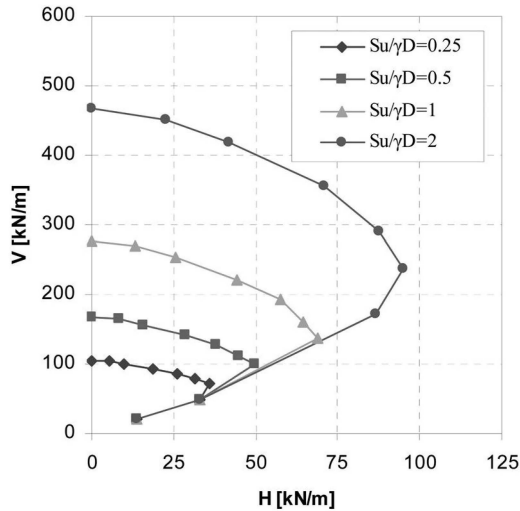


Figure 7. Limitstate:GEO results, VH yield surfaces for strip footing ($B = 2$ m, $D/B = 0.5$ and $\phi = \psi = 35^\circ$).

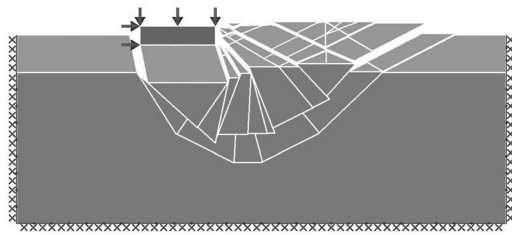


Figure 8. Limitstate:GEO's example of failure mechanism under VH load ($H = 0.3V$, $D/B = 0.5$, $s_u/\gamma D = 0.25$, $\phi' = 35^\circ$).

with friction angle for a given $s_u/\gamma D$. The following relationship fits the data reasonably well:

$$\beta = (0.267\phi' - 25) \ln\left(\frac{s_u}{\gamma D}\right) + (2\phi' - 60) \quad (3)$$

where β and ϕ are both in degrees.

5.3 VH yield surface

An attempt has been made to quantify the influence of the horizontal component of the foundation load as a further development of the load spread concept given in Fig. 1. Figure 9 highlights the horizontal action and reactions on the load spreading sand body (LSB) transferring part of the horizontal load onto its lower potential sliding surface. The need for partial transfer can be inferred from the examination of the intermediate position of the upper portion of the reference (Plaxis) failure envelope in Fig. 2 with respect to either total or zero transfer of horizontal load to the equivalent footing.

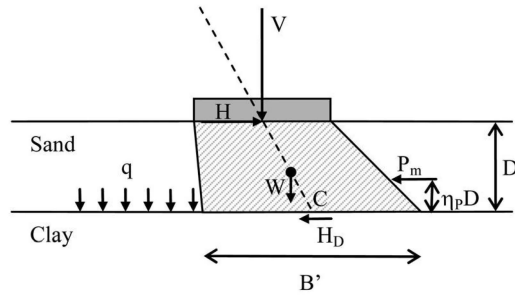


Figure 9. Load transfer mechanism under inclined load.

As can be seen by comparing Fig. 9 with Fig. 1, the following assumptions have been made:

- the LSB centerline, which has the same inclination as the VH load vector, defines the center point C of an equivalent footing on the underlying clay
- the spreading geometry conforms to eq. (3), keeping the equivalent footing width B' resting on top of clay, i.e. $B' = B + 2D \tan\beta$
- passive resistance mobilized along the LSB sides is schematized by a horizontal reaction P_m acting at height $\eta_p D$ above the clay.

The horizontal load H_D transferred to the equivalent footing is obtained by horizontal equilibrium $H_D = H - P_m$ while the moment M_D about point C applied to the lower equivalent footing is modeled by the following expression:

$$M_D = D[\eta_H H - \eta_p P_m - \eta_W (H/V)W] \quad (4)$$

A priori assessments of η_H , η_p , and η_W can be sought by considering the curvature of the funicular thrust line throughout the LSB, a triangular distribution of passive pressures ($\eta_p = 1/3$), and the geometric determination of the centre of mass of the LSB.

The mobilization of P_m follows an initial proportion $\alpha \cdot \pi$ of the applied H according to:

$$\begin{aligned} \pi &= P_{ult} / (P_{ult} + S_{ult}) \\ P_{ult} &= 0.5(K_p - K_a) \gamma H^2 \\ S_{ult} &= s_u B' \end{aligned} \quad (5)$$

The initial rate of P_m mobilization is thus commensurate with the ultimate values of the potentially resisting terms, modulated by the parameter α . One intuitively expects passive resistance to be mobilized preferentially at low H since the base shear is acting at a further distance from the footing than the lateral boundaries of the LSB, especially for large D/B values. In addition, as H increases, displacement compatibility penalizes P_m mobilization that requires a larger displacement than base shear. An analogy is the better known problem of end bearing and friction resistance mobilization of a vertically loaded pile. Based on the above comparison, and allowing for the maximum P_m value to be lower than the reference ultimate

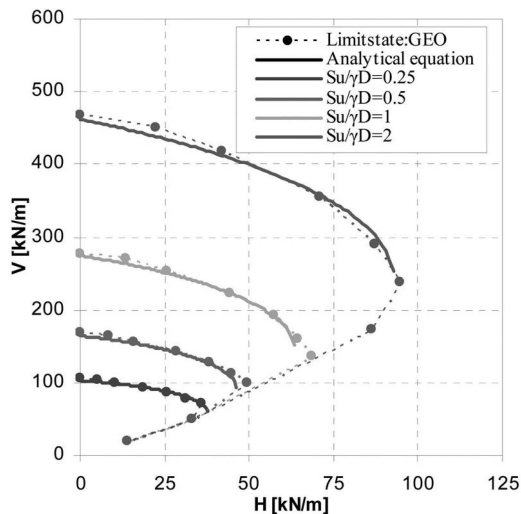


Figure 10. Comparison between analytical equation and Limitstate:GEO results for strip footing ($B = 2$ m, $D/B = 0.5$ and $\phi = \psi = 35^\circ$).

value $P_{\max} = 0.5\alpha\pi H \leq P_{ult}$. P_m is suggested to be mobilized according to the following equation:

$$P_m = \alpha\pi H [1 - (1 - \pi)H / (P_{ult} + S_{ult})] \quad (6)$$

A typical comparison between the proposed simplified approach and LSG calculations is presented in Fig. 10 for the case $D/B = 0.5$ and $\phi' = 35^\circ$. The curves for the different values of $s_u/\gamma D = 0.25, 0.5, 1$ and 2 have all been obtained using the same parameters: $\alpha = 1.1$, η_p and $\eta_w = 1/3$, and $\eta_H = 0.2$. It can be observed that agreement is satisfactory with the upper part of the calculated failure envelope, which was the primary target of the developed approach, i.e. modeling the punch-through mechanism.

Equations presented in this Section have been inserted into proprietary analytical "load spread" method software ISOBARE (Fugro, 2009) for everyday use. This program calculates shallow foundation capacity under general VHM loading on layered soils. Bearing capacity under pure V loading is calculated using the load spread angle deduced from Equation 3. The upper part of the VH yield surface is computed using Equations 4, 5 and 6 while the lower part, where sliding and shear failure in sand dominate, is computed using conventional sand equations (Brinch-Hansen, 1970).

6 DISCUSSION AND CONCLUSIONS

Limitstate:GEO is an appropriate tool to derive VH yield surfaces for surface strip footing on sand over

clay. It is fast and reliable and permitted about 800 analyses in a rigorous and consistent manner.

Based on the results of these numerical simulations, simplified equations are proposed to compute the equivalent load spread angle β and the upper part of the VH yield surface for surface strip footing on sand over uniform clay. These equations have been calibrated in the engineering ranges normally encountered in geotechnical engineering practice.

Given the encouraging results from this first step study assuming infinite strips, the method is being calibrated for other foundation shapes (circles and rectangles) and soil s_u profiles.

REFERENCES

- Brinch Hansen, J. 1970. A revised and extended formula for bearing capacity. *The Danish Geotechnical Institute Bulletin* (28): 5–11.
- Fugro. 2009. *ISOBARE, computer program for shallow foundation capacity on layered soils*.
- Kellezi, L. & Kudsk, G. 2009. Spudcan penetration FE simulation of punch-through for sand over clay. In *12th Jack-Up Platform Conference, London, September 2009*.
- Limitstate. 2009. *Geotechnical software for stability analysis, Version 2*. Sheffield: Limitstate Ltd.
- Loukidis, D. & Salgado, R. 2009. Bearing capacity of strip and circular footings in sand using finite elements. *Computers and Geotechnics* 36(5): 871–879.
- Martin, C.M. 2005. Exact bearing capacity calculations using the method of characteristics. In B. Giovanni & M. Barla (eds.), *Proceedings of the Eleventh International Conference on Computer Methods and Advances in Geomechanics, Torino, Italy, 19–24 June 2005, Vol. 4*: 441–450. Bologna: Patron Editore.
- Michalowski, R.L. & Shi, L. 1995. Bearing capacity of footings over two-layer foundation soils. *Journal of Geotechnical Engineering* 121(5): 421–428.
- Plaxis. 2002. *Finite element code for soil and rock analyses, Version 9*. Delft: Plaxis BV.
- Shiau, J.S., Lyamin, A.V. & Sloan, S.W. 2003. Bearing capacity of a sand layer on clay by finite element analysis. *Canadian Geotechnical Journal* 40(5): 900–915.
- Smith, C. & Gilbert, M. 2007. Application of discontinuity layout optimization to plane plasticity problems. *Proceedings of the Royal Society of London, A* 463(2086): 2461–2484.
- Young, A.G. & Focht (Jr.), J.A. 1981. Subsurface hazards affect mobile jack-up rig operations. *Soundings* (Summer).
- Zienkiewicz, O.C., Humpheson, C. & Lewis, R.W. 1975. Associated and non-associated visco-plasticity and plasticity in soil mechanics. *Géotechnique* 25(4): 671–689.